Mineralogy of a layered gabbro deformed during magmatic crystallization, western Sierra Nevada foothills, California

Robert K. Springer

Department of Geology, Brandon University, Brandon, Manitoba R7A 6A9, Canada

Abstract

In the 162 Ma Pine Hill intrusive complex of northern California, a synformal, layered pyroxenite-gabbro-diorite body, the crystallization sequence and compositional variation of cumulus and intercumulus minerals indicate that magmatic crystallization was characterized by a high initial oxygen fugacity, $\log_{10} f_{O_2}$ in the range of -4 to -9, which allowed the early precipitation of abundant titanomagnetite; the oxygen fugacity decreased less than two log units with crystallization. The magmatic crystallization sequence is ol + aug, ol + aug + mt, ol + aug + mt + pl, ol + aug + mt + pl + opx (inverted from pig) and aug + mt + pl + opx (inverted from pig) + qz. Pigeonite crystallization is evidenced by 001 exsolution lamellae in orthopyroxene of En_{53}. Superimposed upon this sequence are intercumulus minerals, which crystallized from magma trapped within cumulates, and biotite and calcic amphibole, which largely formed from a subsolidus reaction of a residual hydrous fluid phase with primary minerals. Mineral compositional ranges are plagioclase, An_{95} to An_{32}; olivine, Fo_{77} to Fo_{40}; augite, $Ca_{48}Mg_{43}Fe_9$ to $Ca_{43}Mg_{35}Fe_{22}$; Ca-poor pyroxene, $Ca_1Mg_{74}Fe_{25}$ to $Ca_3Mg_{48}Fe_{49}$; Mg/(Mg + Fe + Mn) of calcic amphibole, 0.74 to 0.48; and Mg/(Mg + Fe + Mn) of biotite, 0.78 to 0.45. Prior to complete solidification (>90% crystallized), deformation of the complex coincided with an abrupt decrease in Mg/(Mg + Fe) values for the mafic silicates. This compositional discontinuity is attributed to a decrease in oxygen fugacity of the crystallizing magma caused by an exchange between the fluid phase of adjacent country rock and the fluid phase of the magma during deformation. Prior to deformation of the complex, the Mg/(Mg + Fe) values of the mafic silicates showed the relationship bio > aug > opx > amph > ol whereas after deformation the relationship is aug > opx ≈ bio ≈ amph > ol. Similarities in mineralogy among mafic plutonic rocks of the Pine Hill complex, ophiolites, Alaskan-type complexes, and island-arc plutonic rocks reflect similar conditions of magmatic crystallization. Generation and emplacement of an olivine tholeiite, low in alkalies and high in Ca, within an island-arc environment is proposed for the Pine Hill intrusive complex.

Introduction

Mid-Mesozoic ultramafic to dioritic intrusive complexes and their associated volcanic rocks in the Klamath Mountains and the western Sierra Nevada, California, are part of a petrotectonic association in the western North American Cordillera (Snoke et al., 1982). These complexes are distinguished by (1) dunite, wehrlite, olivine-hornblende clinopyroxenite, olivine gabbro, two-pyroxene gabbro and diorite, and diorite to granodiorite, (2) a complex internal structure, including brecciation and solid flow, (3) a systematic variation in mineral compositions, (4) chemical variations indicative of calc-alkaline magmatism, (5) several episodes of magma emplacement at the same locus, and (6) an orogenic tectonic environment. The structure, petrology, and major-element chemistry of one of these complexes, the Pine Hill intrusive complex, has been previously described (Springer, 1980a, 1980b). This paper describes the mineralogy of the Pine Hill intrusive complex and interprets its magmatic and

subsolidus crystallization in conjunction with the structural evolution of the complex. Comparison of the Pine Hill complex with other complexes in the petrotectonic association as well as with mafic plutonic rocks from established igneous associations is discussed.

Pine Hill intrusive complex

The Middle Jurassic (162 Ma, Saleeby, 1982) Pine Hill intrusive complex is a layered igneous body composed of gabbro with minor pyroxenite and diorite (Springer, 1980a, 1980b) (Fig. 1). Igneous layering forms an asymmetrical synformal structure with a small central area of near-horizontal layering. Primary minerals include olivine, Ca-rich clinopyroxene, Ca-poor pyroxene, plagioclase, oxide minerals, quartz, apatite, and sulfide minerals (Table 1). Late-crystallizing minerals are calcic amphibole and biotite. Secondary minerals that are products of low-temperature alteration of primary and late-crystallizing minerals constitute up to 100% of some gab-
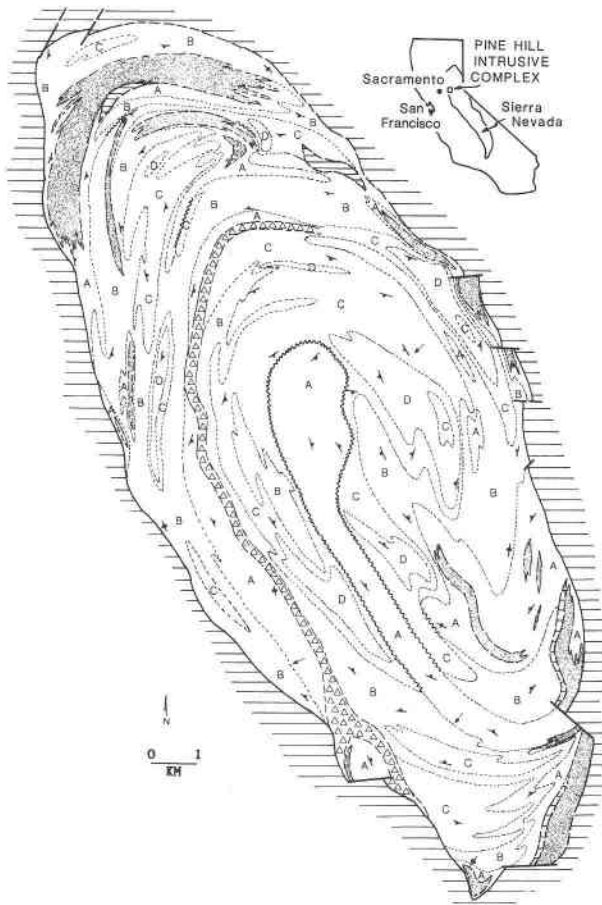
Fig. 1. Geologic map of the Pine Hill intrusive complex, showing the distribution of plagioclase composition in the gabbro. Gabbro types: A = >85 wt% An, B = 70–85 wt% An, C = 55–69 wt% An, D = <55 wt% An. The mixed zone is shown by triangles, and pyroxenite is shown by the dot pattern. Horizontally ruled areas are host rocks. Arrows indicate top determination from outcrop study. Wavy lines show discontinuities in mineral composition. The mineral layering orientations are shown by strike-and-dip symbols.

bros (Springer, 1980b). Gabbro is subdivided into four types based on the wt% An of the plagioclase: A, $>An_{85}$ (18%); B, An_{70} to An_{85} (40%); C, An_{55} to An_{69} (25%); D, $<An_{55}$ (9%). The number in parentheses refers to the portion of the complex composed of this type; pyroxenite makes up the remaining 8% of the complex. The mixed zone is characterized by intercalated lenses of fine-grained, massive gabbro and coarser-grained, massive to slightly foliated gabbro or in some places, by a gabbro breccia. Plagioclase in the mixed zone gabbro is everywhere $<An_{60}$.

A possible model for the structural evolution of the complex (Springer, 1980a, 1980b) involves the formation of layered cumulates in a near horizontal sill-like magma chamber. Accumulation of crystallizing minerals by gravity settling and magmatic currents plus in situ crystallization (McBirney and Noyes, 1979; Irvine, 1980) produced the "stratigraphic" sequence of pyroxenite → interlayered pyroxenite and type A gabbro → type A gabbro → type B gabbro → type C gabbro → type D gabbro. Subsequent external deformation of this sequence prior to complete solidification of the magma produced large-scale brecciation of the more rigid portions and flowage of the less rigid portions. Resultant features include isoclinal folding with axial planes parallel to igneous layering, transposed layering, deformational textures, and mineralogical discontinuities. This deformation also produced the synformal structure of the complex. The internal structure of the complex is not reflected in the structure of the country rock (Springer, 1980b). Adjacent county rock has been contact metamorphosed by the complex (Springer, 1974; Springer and Craig, 1975).

ANALYTICAL TECHNIQUES

Compositional studies of plagioclase, olivine, pyroxenes, oxide minerals, calcic amphibole, and biotite were made utilizing ARL EMX electron microprobes at the University of California, Davis, and the Virginia Polytechnic Institute and State University. All microprobe data were refined using the correction procedures of Rucklidge and Gasparrini (1969) and/or Bence and Albee (1968).

TABLE 1. Average modes of pyroxenite and gabbro

	1	2	3	4	5
Olivine	10 ± 13	13 ± 8	6 ± 4	4 ± 3	2 ± 2
Ca-rich clinopyroxene	69 ± 22	15 ± 15	28 ± 12	22 ± 5	13 ± 5
Ca-poor pyroxene	<1	1 ± 1	2 ± 2	4 ± 2	6 ± 5
Plagioclase	<1	64 ± 14	55 ± 13	63 ± 7	66 ± 4
Oxide minerals	2 ± 5	3 ± 3	4 ± 2	4 ± 1	4 ± 1
Quartz	0	0	0	0	<1
Apatite	0	0	<1	<1	<1
Calcic amphibole	4 ± 5	3 ± 4	5 ± 7	3 ± 6	1 ± 2
Biotite	<1	<1	1 ± 1	1 ± 1	1 ± 1
Secondary minerals*	15 ± 17	1 ± 4	<1	<1	1 ± 2

Note: Columns are averages and standard deviations for (1) 43 pyroxenites, (2) 27 type A gabbro, (3) 33 type B gabbro, (4) 28 type C gabbro, (5) 19 type D gabbro.

* Secondary minerals include tremolite-actinolite, clinozoisite-epidote, chlorite, serpentine minerals, talc, iron oxide minerals, sericite, carbonate minerals.
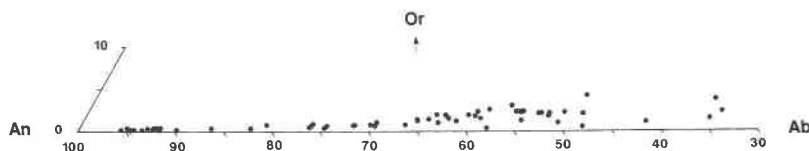
Fig. 2.   An-Ab-Or plot of plagioclase compositions from the Pine Hill intrusive complex.

To determine the variation of plagioclase composition within a single hand specimen, the chemical composition of plagioclase separates was determined by three methods, (1) electron microprobe, (2) refractive index of the plagioclase glass, and (3) X-ray fluorescence analysis. Plagioclase compositions determined by the three methods are statistically identical. This feature suggests that the smaller sample size, i.e., 6–10 spots on 3–4 grains used in electron-microprobe analysis versus hundreds of grains used in X-ray fluorescence analysis, adequately reflects the average composition of plagioclase in a single hand specimen. Rapid determination of plagioclase composition for this study was made using wt% An = $[(\Gamma + 0.798)/0.253]$, where $\Gamma = 2\theta(131 - 1\bar{3}1) - 2\theta(1\bar{3}1 - 220)$. Increasing substitution of K resulted in lower values for Γ.

To determine outcrop variation in the composition and Γ of plagioclase, four hand specimens from an outcrop in each of the four gabbro types were selected perpendicular to igneous layering. There is a highly significant difference in Γ among outcrops from the four types but more important, a significant difference within a single outcrop. To determine whether the variation within a single outcrop could be related to modal layering, sampling perpendicular to layering over a 70-m interval with additional sampling with the 70-m interval over 10 m, and over 1 m, was carried out. Variation in Γ and plagioclase composition indicates a top direction consistent with the regional top direction suggested by plagioclase compositions from nearby outcrops (Fig 1).

MINERALOGY

Using the compositional range of plagioclase (Fig. 2) as a measure of the degree of magmatic crystallization in the Pine Hill complex, the compositions of the mafic silicates and oxide minerals are discussed relative to the composition of their coexisting plagioclase. The relative proportions of the five mappable units (pyroxenite; gabbro types A, B, C, and D) suggest that all rock types resulting from magmatic crystallization are represented within the outcrop of the complex.

Plagioclase

Plagioclase occurs as an intercumulus mineral in pyroxenite and as a cumulus mineral in gabbro. Plagioclase grains in most gabbro have undergone recrystallization and/or granulation. Plagioclase morphology ranges from subhedral elongate grains unaffected by fracturing or recrystallization through anhedral, but elongate grains to fine-grained equant anhedral grains. Plagioclase deformation is generally more common with decreasing anorthite content of the plagioclase. Mechanical or deformational twinning of plagioclase (Smith, 1974, v. 2, p.

345) is common. Similar deformational textures in plutonic igneous rocks have been reported, e.g., Kehlenbeck (1972), Moore (1973), and Jorgenson (1979).

No compositional differences between deformed and undeformed plagioclase were detected. Compositional zoning is optically observed only in plagioclases of $<An_{60}$. Exsolution of K-feldspar spindle-shaped blebs, up to 50 μm in length, occurs near grain boundaries, near fractures, or within twin lamellae in plagioclase of $<An_{55}$. The Fe content of plagioclase, 0.04–0.13 wt%, increases slightly with increasing An content.

Olivine

Olivine exhibits a modal decrease from near 20% in pyroxenite and type A gabbro to zero percent in gabbro containing plagioclase near An_{35} (Table 1). Olivine exhibits deformational features such as undulose extinction, deformation lamellae, and mortar texture. Inclusions in olivine are rare, but oriented inclusions of symplectic iron oxide minerals, as described by Moseley (1984), are observed in olivine from certain pyroxenites and type A gabbro. Ca-poor pyroxene and vermicular iron oxide minerals are commonly associated with olivine in gabbro with plagioclase of $<An_{90}$. Olivine with partial rims of Ca-poor pyroxene without vermicular iron oxide minerals is present in most gabbro, but rarely in pyroxenite.

Olivine shows an apparently continuous Fe-enrichment trend from Fo_{77} to Fo_{40} (Table 2) with a sympathetic increase in MnO. Chemical zoning within olivine grains is minor, $<2\%$ Fo variation.

Ca-rich clinopyroxene

Ca-rich clinopyroxene, mainly augite, generally occurs as a cumulus mineral. Composite grains in which irregular blebs of Ca-poor pyroxene protrude into or partially rim augite grains, are common in gabbro of the Pine Hill complex. These composite grains are attributed to granule exsolution of Ca-poor pyroxene from augite (Best and Mercy, 1967; Lindsley and Andersen, 1983) rather than an epitaxic relationship between the two pyroxenes (Tarney, 1969). Exsolution lamellae of orthopyroxene, up to 40 μm thick and parallel to the 100 plane of the host augite, are present in augite of gabbro with plagioclase of An_{90} to An_{40}. Irregular blebs of orthopyroxene in optical continuity with associated 100 lamellae are common in augite. Only in gabbro with plagioclase of An_{65} to An_{32} were two sets of pigeonite exsolution lamellae in augite observed, (1) "001" lamellae at an angle of near 106° with

TABLE 2. Representative electron-microprobe analyses of olivines

	SS147	RKS40	PH58	PH120	JB7	PH168	PH115
SiO_2	38.65	37.95	38.37	37.36	36.25	34.49	33.45
TiO_2	0.01	0.01	0.06	0.02	0.02	0.02	0.03
Al_2O_3	0.06	0.04	0.00	0.00	0.08	0.06	0.11
FeO*	22.56	24.93	26.06	29.32	33.96	43.52	46.44
MnO	0.38	0.44	0.35	0.42	0.72	0.83	1.00
MgO	39.42	36.17	37.12	33.45	29.05	21.48	18.12
CaO	0.06	0.05	0.03	0.05	0.07	0.08	0.11
	101.14	99.59	101.99	100.62	100.15	100.48	99.26
	Number of ions on the basis of 4 oxygens						
Si	0.993	1.004	0.995	1.000	0.999	0.997	0.998
Ti			0.001				0.001
Al	0.002	0.001			0.002	0.002	0.004
Fe	0.485	0.551	0.565	0.656	0.783	1.051	1.158
Mn	0.008	0.010	0.008	0.010	0.017	0.020	0.025
Mg	1.512	1.427	1.434	1.334	1.193	0.925	0.806
Ca	0.002	0.002	0.001	0.001	0.002	0.002	0.004
Mg/(Mg + Fe + Mn)	0.754	0.718	0.714	0.667	0.599	0.463	0.405

* Total Fe determined as FeO.

the c axis of augite and up to 5 μm thick and (2) "001" lamellae at an angle of near 112° with the c axis and up to 1 μm thick. Exsolution lamellae optically identified in four augites correlated with lamellae in X-ray precession photographs of these augites. Exsolution lamellae of pigeonite in Pine Hill augites correlate with Pig II and Pig III lamellae of Robinson et al. (1977), which nucleate at approximately 800 and 600 °C, respectively. In Pine Hill augites, the absence of Pig I and Pig "100" lamellae, which nucleate at approximately 1000 and 850 °C, respectively, are attributed to down-temperature migration of pigeonite from these lamellae to form irregular grains within augite or at its boundaries. Plates and needles of iron oxide minerals in augite are oriented approximately parallel to the (100) and (001) planes of the host augite. The iron oxide inclusions decrease in abundance with decreasing anorthite content of the coexisting plagioclase.

Although there has been subsolidus equilibration of the Pine Hill pyroxenes, compositional trends are discernible (Table 3, Fig. 3). Trend A in which En remains relatively constant between 42.9 and 39.6 and Wo decreases from 49.3 to 41.7 represents the compositions of augite that did not coprecipitate with Ca-poor pyroxene. Trend B in which En decreases from 42.0 to 34.9 and Wo increases slightly from 41.7 to 44.2 represents those that did precipitate the Ca-poor pyroxene. The Al_2O_3 content of augite shows a decrease, 4.39 to 0.80 wt%, with increasing Fe content of augite. TiO_2 content also decreases, 0.94 to 0.22 wt%, with increasing Fe content of augite, whereas MnO content shows an increase, 0.13 to 0.66 wt%. Although Na_2O and calculated Fe_2O_3 contents show no trend with the Fe content of augite, the Na_2O content increases with increasing Fe_2O_3 content. Correlation of Mg/(Mg + Fe) with anorthite content for coexisting augite and plagioclase shows minor Fe enrichment in augite (Fig. 4). Plots of Mg/(Mg + Fe) vs. anorthite content for olivine and Ca-poor pyroxene show a similar relationship.

Ca-poor pyroxene

Ca-poor pyroxene occurs as (1) partial rims around olivine, (2) symplectites with vermicular iron oxide minerals, (3) composite grains with augite, and (4) separate cumulus or intercumulus grains. The first occurrence is observed in some pyroxenite and most olivine-bearing gabbro; the second, in gabbro containing plagioclase of An_{95} to An_{40}; the third, in gabbro containing plagioclase of An_{95} to An_{32}; the fourth, in gabbro containing plagioclase of $<An_{80}$. Symplectites of Ca-poor pyroxene with vermicular iron oxide minerals occur as single grains of Ca-poor pyroxene enclosing vermicular iron oxide minerals or as an aggregate of equant anhedral grains of Ca-poor pyroxene with vermicular iron oxide minerals crosscutting grain boundaries but not extending beyond the aggregate boundary. These symplectites have formed after the partial rims of Ca-poor pyroxene as these rims are observed to border aggregates of Ca-poor pyroxene grains with vermicular iron oxide minerals. Their formation occurred prior to the crystallization of calcic amphibole and biotite as these minerals show a replacement relationship with these symplectites.

Ca-poor pyroxenes commonly exhibit exsolution lamellae of augite up to 0.02 mm thick and parallel to 100. Exsolution lamellae up to 0.02 mm thick and parallel to the "001" plane of the host Ca-poor pyroxene were observed in gabbro with plagioclase of An_{53}. As textural features show a gradation from continuous 100 or "001" lamellae to discontinuous 100 or "001" lamellae to random irregular blebs, down-temperature migration of exsolved augite has largely obliterated most higher-temperature exsolution textures (Lindsley and Andersen, 1983). Compositional, textural, and single-crystal X-ray studies show that the Ca-poor pyroxene in all four occurrences is orthopyroxene and that the Ca-poor pyroxene coexisting with plagioclase of An_{53} was originally pigeonite that later inverted to orthopyroxene.
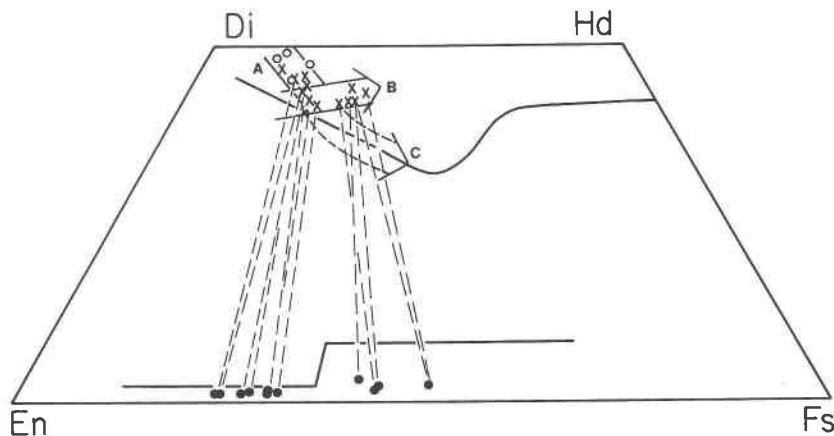
Fig. 3. Compositions of pyroxenes from the Pine Hill intrusive complex plotted on the pyroxene quadrilateral. Crystallization trends: A, cumulus augite; B, cumulus augite with cumulus Ca-poor pyroxene; C, same as B but augite corrected for exsolution. Solid lines represent the trend for pyroxenes from the Skaergaard intrusion (Wager and Brown, 1967).

Although subsolidus exsolution of augite has altered the composition of the Ca-poor pyroxenes (Table 3), their compositions correlate with those of augite (Fig. 3). Al_2O_3 content decreases from 1.71 to 0.39 wt% with decreasing $Mg/(Mg + Fe)$, similar to augite. MnO content increases with decreasing $Mg/(Mg + Fe)$.

Equilibrium temperatures for ten pairs of cumulus augite and Ca-poor pyroxene coexisting with plagioclase ranging from An_{70} to An_{32} in the complex were calculated using various pyroxene geothermometers: 888 ± 47 °C (Wood and Banno, 1973), 919 ± 49 °C (Wells, 1977), 912 ± 61 °C and 996 ± 28 °C (low T and high T of the transfer equation, Kretz, 1982), and a range of 1484 to 720 °C (exchange equation, Kretz, 1982). Three pairs yielded a range of 950 to 750 °C using the geothermometer of Lindsley (1983). These calculated temperatures are largely subsolidus equilibrium temperatures. Using the chemical composition of the coexisting pyroxenes and the modal percent of exsolved pyroxene in the host pyroxene, a temperature of magmatic crystallization of near 1100 °C (Lindsley, 1983) was determined. These data suggest that in the pyroxene quadrilateral (Fig. 3), trend B probably represents a subsolidus trend whereas trends A and C approximate the magmatic crystallization path of augite in the complex.

Oxide minerals

Oxide minerals (titaniferous magnetite and ilmenite) are present in gabbro but only rarely in pyroxenite except for the pyroxenite body at the southern end of the complex (Fig. 1). In rhythmically layered gabbro containing plagioclase of $>An_{85}$, layers up to one-third meter thick contain up to 30% and, in one instance, 100% iron oxide minerals.

Titaniferous magnetite, which occurs as a cumulus and intercumulus mineral as well as vermicular intergrowths with Ca-poor pyroxene, is always associated with ilmenite. Ilmenite occurs as coarse lamellae, fine trellis inter-

growths, and irregular grains adjacent to or within magnetite, as described by Buddington and Lindsley (1964). All three occurrences, in various combinations, are found in gabbro with plagioclase of all compositions. The modal ratio of ilmenite to magnetite increases with decreasing anorthite content of the coexisting plagioclase. Granules of ilmenite increase from <1% of total iron oxide min-
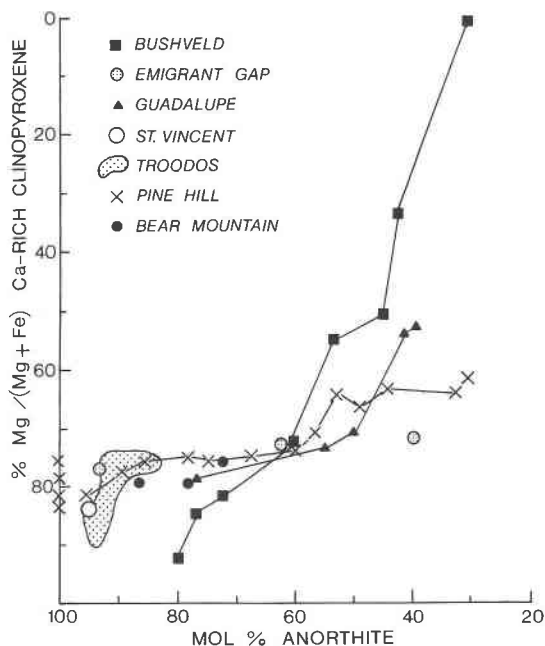

Fig. 4. Compositions of coexisting Ca-rich clinopyroxene and plagioclase from the Pine Hill intrusive complex compared to those from other plutonic rocks. Pyroxenes from pyroxenites are assigned an anorthite content of 100. Sources of data: Bushveld (Wager and Brown, 1967), Emigrant Gap (James, 1971), Guadalupe (Best and Mercy, 1967), St. Vincent (Lewis, 1973b), Troodos (Allen, 1975), Bear Mountain (Snoke et al., 1981).

TABLE 3. Representative electron-microprobe analyses of pyroxenes

	SS147	RSK40	PH58	PH120	JB7	PH168	PH115	SS135	PH58
SiO_2	51.80	51.39	51.00	52.33	50.69	51.10	51.06	52.55	54.29
TiO_2	0.76	0.54	0.58	0.49	0.51	0.48	0.41	0.22	0.12
Al_2O_3	4.22	4.39	3.53	2.89	3.24	2.39	2.19	0.80	1.63
FeO^*	5.39	6.02	8.12	8.71	8.46	12.42	12.74	12.04	16.56
MnO	0.14	0.18	0.19	0.22	0.30	0.41	0.47	0.50	0.34
MgO	15.18	14.80	14.10	14.52	14.05	12.71	12.42	12.18	27.70
CaO	23.86	22.52	22.00	20.78	20.94	20.33	20.17	20.81	0.58
Na_2O	0.30	0.49	0.30	0.37	1.07	0.73	0.81	0.34	0.00
	101.65	100.33	99.82	100.31	99.26	100.57	100.27	99.44	101.23
				Number of ions on the basis of 6 oxygens					
Si	1.880	1.889	1.901	1.935	1.905	1.924	1.932	1.994	1.943
Al	0.120	0.111	0.099	0.065	0.095	0.076	0.068	0.006	0.057
[Z]	2.000	2.000	2.000	2.000	2.000	2.000	2.000	2.000	2.000
Al	0.061	0.079	0.056	0.061	0.049	0.030	0.030	0.030	0.012
Ti	0.021	0.015	0.016	0.014	0.014	0.014	0.012	0.006	0.003
Fe	0.164	0.185	0.253	0.269	0.266	0.391	0.403	0.382	0.496
Mn	0.004	0.006	0.006	0.007	0.010	0.031	0.015	0.016	0.010
Mg	0.821	0.811	0.783	0.800	0.787	0.713	0.700	0.689	1.477
Ca	0.928	0.887	0.879	0.823	0.843	0.820	0.818	0.846	0.022
Na	0.021	0.035	0.022	0.027	0.078	0.053	0.059	0.025	0.000
[X,Y]	2.019	2.018	2.016	2.001	2.047	2.036	2.037	1.994	2.020
Mg/(Mg + Fe + Mn)	0.830	0.809	0.751	0.743	0.740	0.638	0.626	0.634	0.745
Ca	48.5	47.1	45.9	43.5	44.5	42.6	42.6	44.1	1.1
Mg	42.9	43.1	40.9	42.3	41.5	37.1	36.4	35.9	74.0
Fe	8.6	9.8	13.2	14.2	14.0	20.3	21.0	19.9	24.9

* Total Fe determined as FeO.

erals in pyroxenite and gabbro with plagioclase of $>An_{85}$ to near 30% in gabbro with plagioclase near An_{32}. Isolated grains of ilmenite were not observed. Ilmenite in all occurrences is optically and chemically homogeneous. Pleonaste occurs as lamellae parallel to the octahedral planes of magnetite and as irregular grains concentrated at magnetite grain boundaries and within coarse ilmenite blades. Pleonaste becomes less abundant with decreasing anorthite content of the coexisting plagioclase.

Compositional trends in magnetite with respect to the anorthite content of the coexisting plagioclase are discernible for TiO_2, Al_2O_3, Fe_2O_3, and FeO (Table 4). TiO_2 in magnetite increases from <1 wt% in pyroxenite to >11 wt% in gabbro with plagioclase of An_{44} but drops to <1.5 wt% in gabbro with plagioclase of $<An_{35}$. TiO_2 values for two magnetites (FO13, JD82; Table 4) appear anomalously high. McBirney and Noyes (1979) have shown that there is sympathetic relationship between the modal abundance and the chemical composition of iron oxide minerals in layered gabbro (i.e., high TiO_2 and MgO con-

tent in magnetite from oxide-rich layers). The average modal amount of iron oxide minerals in the complex is $<5\%$ but FO13 and JD82 contain $\sim 30\%$ and 100% oxide minerals, respectively. MgO content of these magnetites and their coexisting ilmenites (Tables 4, 5) are the highest of all magnetite and ilmenite in the complex.

The Fe_2O_3 content of magnetite, which decreases with decreasing anorthite content of the coexisting plagioclase, shows an inverse relationship to that of FeO and TiO_2, characteristic of the Fe_2TiO_4-Fe_3O_4 series (Lindsley, 1976). Al_2O_3 increases with decreasing anorthite content. Because the abundance of exsolution lamellae of pleonaste in magnetite decreases with decreasing anorthite content, the Al_2O_3 trend possibly reflects the degree of pleonaste exsolution rather than magmatic fractionation.

Similar to the TiO_2 content, the FeO and Al_2O_3 contents of magnetite from gabbro with plagioclase of $<An_{35}$ are distinctly lower than those in gabbro from the rest of the complex, whereas the Fe_2O_3 content is distinctly higher. Cr_2O_3 shows a general decrease with decreasing

TABLE 4. Representative electron-microprobe analyses of magnetites and a pleonaste

	FO13	FO13**	RKS84	JD82	JB7	PH168	PH115	RKS18
TiO_2	7.13	0.05	3.12	4.09	6.43	11.09	11.35	1.34
Al_2O_3	1.94	58.40	0.92	0.82	2.34	3.22	3.14	0.59
Cr_2O_3	0.06	0.04	0.25	0.28	0.04	0.09	0.04	0.03
$Fe_2O_3^*$	55.20	6.17	62.58	60.07	55.29	44.37	43.98	66.01
FeO^*	34.97	22.74	33.59	33.28	37.48	41.16	41.38	32.08
MnO	0.51	0.24	0.39	0.61	0.41	0.54	0.65	0.45
MgO	2.00	11.82	0.31	0.67	0.12	0.29	0.22	0.00
	101.81	99.46	101.16	99.82	102.11	100.76	100.77	100.50

* Recalculation of Fe_2O_3 and FeO after Carmichael (1967), Anderson (1968), Lindsley and Spencer (1982), and Stormer (1983).
** Pleonaste.

TABLE 3—*Continued*

PH120	JB7	PH168	PH115	SS135
54.28	52.87	51.54	51.19	51.44
0.15	0.14	0.20	0.19	0.09
1.58	1.77	1.10	1.20	0.39
17.70	19.27	24.96	26.15	30.24
0.41	0.59	0.70	0.83	1.25
25.61	24.07	19.20	18.13	16.27
0.65	0.80	1.59	0.97	1.13
0.00	0.02	0.01	0.07	0.02
100.38	99.55	99.32	98.74	100.82
Number of ions on the basis of 6 oxygens				
1.967	1.953	1.968	1.975	1.984
0.033	0.047	0.032	0.025	0.016
2.000	2.000	2.000	2.000	2.000
0.034	0.030	0.018	0.030	0.002
0.004	0.004	0.006	0.006	0.003
0.536	0.595	0.797	0.844	0.976
0.013	0.018	0.023	0.027	0.041
1.383	1.325	1.093	1.043	0.935
0.025	0.032	0.065	0.040	0.047
0.000	0.001	0.001	0.005	0.001
1.995	2.006	2.002	1.994	2.005
0.716	0.684	0.571	0.545	0.479
1.3	1.6	3.3	2.1	2.4
71.1	67.9	55.9	54.1	47.8
27.6	30.5	40.8	43.8	49.8

anorthite content. Although magnetite contains significant amounts of MgO and MnO, 0.00 to 2.00 wt% and 0.08 to 0.65 wt%, respectively, no regular variation with anorthite content is discernible. No compositional trends in ilmenite with respect to the anorthite content of the coexisting plagioclase are discernible, but the MgO and MnO contents of ilmenite exhibit a direct and inverse relationship, respectively, with those of magnetite.

Using the ulvöspinel and ilmenite components (Carmichael, 1967; Lindsley and Spencer, 1982; Stormer, 1983) calculated from the compositions of 12 magnetite and ilmenite pairs from pyroxenite and all four types of gabbro and the temperature model of Spencer and Lindsley (1981), and temperature range of 516 to 648 °C and a $\log_{10} f_{O_2}$ range of -18.4 to -25.6 were determined. All textural and compositional features of the oxide minerals indicate that subsolidus oxidation-exsolution of a primary titanomagnetite produced a titaniferous magnetite with associated ilmenite and pleonaste.

Calcic amphibole

Calcic amphibole occurs as partial rims around primary minerals, especially pyroxene and iron oxide minerals, and as irregular patches within pyroxene. In gabbro with abundant deformational textures, anhedral equant grains of calcic amphibole are typical. Generally calcic amphibole forms <10% of the mafic minerals in any pyroxenite or gabbro, but in certain gabbros, it constitutes nearly 100% of the mafic minerals. Calcic amphibole exhibits pleochroism of X = tan, Y = medium brown, and Z = dark brown to reddish brown in most gabbro, but a pleochroism of X = colorless, Y = pale green, and Z = medium green in most pyroxenite. Calcic amphibole and biotite, which are commonly associated in the same rock, appear to have crystallized at the same time. Whether calcic amphibole and biotite occur together or separately depends largely on the bulk composition. For example, in gabbro with plagioclase near An_{50}, if $K_2O > 0.55$ wt%, only biotite is present; if $K_2O = 0.30$–0.55 wt%, biotite and calcic amphibole are present; if $K_2O < 0.30$ wt%, only calcic amphibole is present.

Using the nomenclature of Leake (1978), the chemical compositions of the calcic amphiboles (Table 6, Fig. 5) show a compositional gap between those from gabbro with plagioclase of $<An_{35}$ and all other calcic amphiboles in the complex. This discontinuity coincides with the first appearance of quartz. Pargasite, which is not stable with quartz (Gilbert et al., 1982), is replaced by ferro-edenitic hornblende. Na + K increases with increasing Fe content in the calcic amphiboles prior to the crystallization of quartz. The Mg/(Mg + Fe) of calcic amphibole decreases with decreasing anorthite content of the coexisting plagioclase (Fig. 6).

Biotite

The occurrence and textural features of biotite are similar to those of calcic amphibole. It exhibits a pleochroism of X = pale brown and Y = Z = dark red brown. Biotite shows a general decrease in Mg/(Mg + Fe) with decreasing anorthite content of the coexisting plagioclase (Table 7, Fig. 6). Biotite is the most magnesian mineral in gabbro with plagioclase of $>An_{60}$ but becomes one of the most Fe-rich minerals, second only to olivine, in gabbro with plagioclase of $<An_{50}$. Alumina generally decreases with decreasing Mg/(Mg + Fe), whereas TiO_2 in-

TABLE 5. Representative electron-microprobe analyses of ilmenites

	FO13	RKS84	JD82	JB7	PH168	PH115	RKS18
TiO_2	51.95	53.26	54.78	52.19	51.73	51.98	51.67
Al_2O_3	0.05	0.09	0.07	0.11	0.11	0.11	0.07
Cr_2O_3	0.00	0.03	0.00	0.00	0.00	0.00	0.00
$Fe_2O_3^*$	5.01	1.92	1.87	1.85	2.55	2.62	4.68
FeO^*	32.42	41.86	38.00	44.10	43.18	43.49	40.49
MnO	1.08	2.47	2.00	2.34	1.18	1.58	5.85
MgO	7.41	1.98	5.18	0.26	1.20	0.93	0.02
	97.92	101.61	101.91	100.75	99.96	100.70	102.76

* Recalculation of Fe_2O_3 and FeO after Carmichael (1967), Anderson (1968), Lindsley and Spencer (1982), and Stormer (1983).
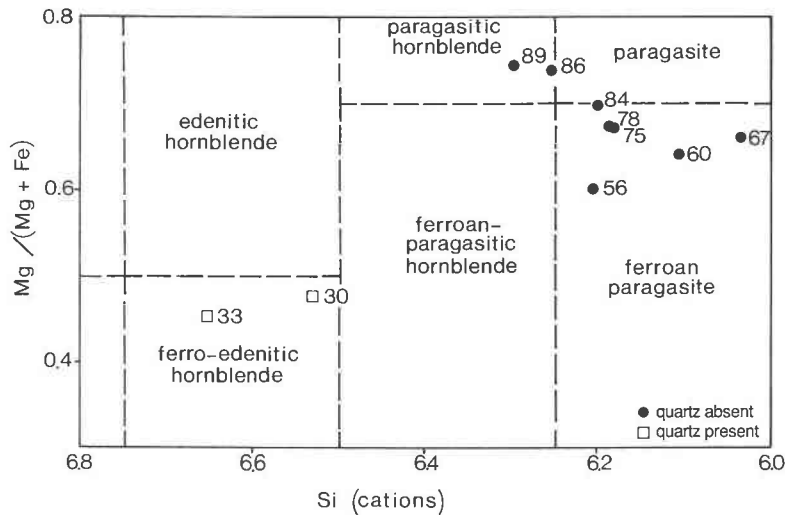
Fig. 5.   Variation of Mg/(Mg + Fe) with Si for calcic amphiboles in the Pine Hill intrusive complex. Numbers refer to the anorthite content of the coexisting plagioclase.

creases. Higher values of Na_2O occur in biotite coexisting with plagioclase of $>An_{60}$.

Quartz, apatite, and sulfide minerals

Quartz was observed in only three gabbros (Table 1), which occur in either the mixed zone or the zone in which plagioclase compositions are $<An_{55}$. It occurs as anhedral grains interstitial to primary minerals, except in one gabbro where it occurs in fractures crosscutting plagioclase grains. Plagioclase coexisting with quartz is the most sodic, $<An_{35}$, in the complex.

Apatite first appears in gabbro containing plagioclase near An_{70} (Table 1). It commonly occurs as inclusions of euhedral crystals in plagioclase, but can occur as anhedral grains up to 1 mm in diameter in some gabbros.

As only trace amounts of sulfide minerals are present in the complex, no study of these minerals was undertaken.

PETROGENESIS

Crystallization sequence

Using the anorthite content of cumulus plagioclase as a measure of the degree of magmatic crystallization, the stratigraphic succession of primary mineral assemblages is aug + ol, aug + ol + mt, pl + aug + ol + mt, pl + aug + opx (inverted from pig) + ol + mt, pl + aug + opx (inverted from pig) + mt, pl + aug + opx (inverted from pig) + mt + qz. Pigeonite is the crystallizing Ca-poor pyroxene near En_{53}, but the compositional limits of pigeonite crystallization are not known. Superimposed on these assemblages are Ca-poor pyroxene, iron oxide minerals, calcic amphibole, and biotite, none of which crystallized directly from the main body of magma, but from isolated intercumulus magma or by a subsolidus reaction. Experimental studies of basalts under variable oxygen fugacity (Roeder and Osborn, 1966; Presnall, 1966; Osborn, 1979) best illustrate the crystallization sequence in the Pine Hill complex. Magnetite crystallization, which occurs after that of olivine and augite, is closely followed by that of plagioclase, and results in the simultaneous crystallization of olivine, augite, magnetite, and plagioclase. Olivine is totally consumed as plagioclase nears An_{40}, so the common assemblage pl + ol + aug + Ca-poor pyroxene + mt changes to aug + Ca-poor pyroxene + mt + pl ± qz.

Evidence for adcumulus growth during magmatic crystallization of the Pine Hill complex is the lack of chemical zoning in the primary minerals, and the occurrence of monomineralic layers of titanomagnetite with <5% interstitial silicate minerals and up to one-third meter thick, and layers of olivine clinopyroxenite with less than 5% interstitial plagioclase (Wager et al., 1960; Morse, 1980, p. 240).
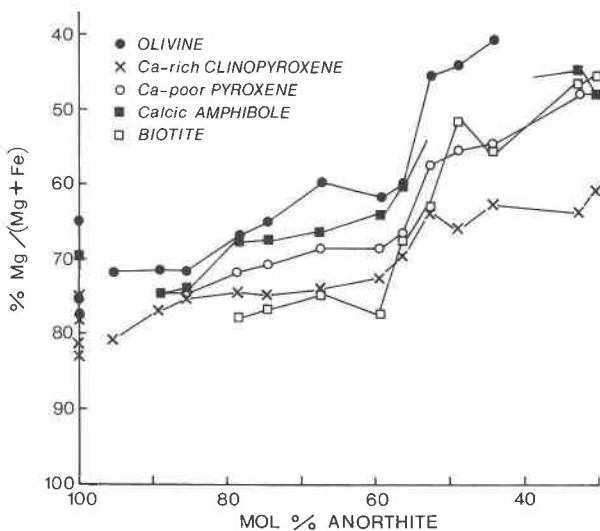

Fig. 6.   Variation of Mg/(Mg + Fe) in mafic silicates with plagioclase composition in the Pine Hill intrusive complex.

TABLE 6. Representative electron-microprobe analyses of calcic amphiboles

	RKS84	PH58	PH120	SS129	SS135
SiO_2	43.15	42.94	42.15	42.05	43.71
TiO_2	2.15	1.83	2.67	2.63	1.90
Al_2O_3	12.63	13.08	12.97	12.61	8.87
FeO*	9.19	9.41	11.44	14.21	20.19
MnO	0.20	0.08	0.10	0.20	0.33
MgO	14.99	14.93	13.20	11.96	9.49
CaO	12.05	12.20	11.92	11.40	11.03
Na_2O	2.57	2.23	2.48	2.73	1.67
K_2O	0.16	1.08	1.38	1.06	0.55
	97.09	97.78	98.31	98.85	97.74
Number of ions on the basis of 23 oxygens					
Si	6.299	6.256	6.189	6.209	6.655
Al	1.701	1.744	1.811	1.791	1.345
[Z]	8.000	8.000	8.000	8.000	8.000
Al	0.472	0.502	0.434	0.404	0.247
Ti	0.236	0.201	0.295	0.292	0.218
Fe	1.122	1.147	1.405	1.755	2.571
Mn	0.025	0.010	0.012	0.025	0.043
Mg	3.261	3.242	2.889	2.632	2.153
[X, Y]	5.116	5.102	5.035	5.108	5.232
Ca	1.885	1.905	1.876	1.804	1.800
Na	0.727	0.630	0.706	0.782	0.493
K	0.030	0.200	0.259	0.200	0.107
[W]	2.642	2.735	2.841	2.786	2.400
Mg/(Mg + Fe + Mn)	0.740	0.737	0.671	0.597	0.452

* Total Fe determined as FeO.

TABLE 7. Representative electron-microprobe analyses of biotites

	PH120	JB7	PH168	PH115	SS135
SiO_2	37.94	37.08	37.81	36.55	36.58
TiO_2	3.11	3.36	4.50	5.84	4.79
Al_2O_3	16.54	16.63	15.17	14.64	13.37
FeO*	9.28	11.67	15.54	18.21	21.32
MnO	0.02	0.06	0.07	0.11	0.12
MgO	18.18	19.01	14.74	12.76	10.39
CaO	0.08	0.12	0.07	0.05	0.06
Na_2O	0.32	0.31	0.06	0.00	0.09
K_2O	9.27	8.67	9.41	9.71	9.12
	94.74	96.91	97.37	97.87	95.84
Number of ions on the basis of 22 oxygens					
Si	5.528	5.342	5.510	5.420	5.612
Al	2.472	2.658	2.490	2.559	2.388
[Z]	8.000	8.000	8.000	7.979	8.000
Al	0.370	0.166	0.174		0.031
Ti	0.341	0.365	0.493	0.651	0.552
Fe	1.131	1.406	1.894	2.258	2.735
Mn	0.003	0.007	0.009	0.014	0.016
Mg	3.948	4.081	3.201	2.820	2.376
[Y]	5.793	6.025	5.771	5.743	5.710
Ca	0.012	0.018	0.011	0.008	0.010
Na	0.091	0.087	0.018		0.028
K	1.723	1.593	1.750	1.827	1.785
[X]	1.826	1.698	1.789	1.835	1.823
Mg/(Mg + Fe + Mn)	0.777	0.743	0.628	0.555	0.465

* Total Fe determined as FeO.

Crystal sedimentation eventually prohibits effective diffusion between the magma body and intercumulus magma, and a certain amount of intercumulus magma is trapped within the cumulates. Partial rims of Ca-poor pyroxene on olivine are attributed to a reaction between olivine and trapped intercumulus magma, because the rims of Ca-poor pyroxene have formed in pyroxenite and Type A gabbro prior to the direct precipitation of Ca-poor pyroxene from the main body of magma. Crystallization of phases directly from the trapped magma, along with crystallization of phases resulting from the reaction of this magma with cumulus minerals, would cause depletion and concentration of elements within the trapped magma similar to fractional crystallization of the main body of magma. On the basis of textural evidence—such as irregular patches of hydrous minerals within primary minerals, lack of primary accessory minerals with hydrous minerals, and Ca-poor pyroxene with vermicular titanomagnetite rimmed by Ca-poor pyroxene—the alteration of olivine to Ca-poor pyroxene and vermicular titanomagnetite and the formation of calcic amphibole and biotite probably occurred in equilibrium with an intercumulus hydrous fluid phase rather than an intercumulus silicate melt. Using calculated temperatures of crystallization and similar textures, intercumulus hornblende in similar gabbros is attributed to a high-temperature subsolidus reaction between a hydrous fluid phase and primary minerals (Otten, 1984; Morrison et al., 1986).

Conditions of crystallization

Magmatic crystallization of the Pine Hill complex occurred at a total pressure of less than 3 kbar on the basis of contact-metamorphic mineral assemblages (Springer, 1974, 1980b). The total pressure can also be estimated from the chronologic sequence of cumulus phases. As the stability of plagioclase is suppressed 250 °C with increasing water pressure between 2 and 8 kbar (Yoder and Tilley, 1962; Holloway and Burnham, 1972), a total pressure near 2.5 kbar would be indicated for the Pine Hill complex.

Under the most oxidizing conditions, i.e., oxygen fugacity controlled by the HM (hematite-magnetite) buffer, melting relations of basalts show that titanomagnetite is one of the highest-temperature liquidus phases (Hamilton et al., 1964; Holloway and Burnham, 1972; Helz, 1973), whereas under a lower oxygen fugacity as controlled by the NNO (Ni-NiO) buffer, titanomagnetite crystallizes after olivine and Ca-rich clinopyroxene. Under still lower oxidizing conditions, i.e., the FMQ (fayalite-magnetite-quartz) buffer, ilmenite is a high-temperature liquidus phase. The Pine Hill complex largely crystallized under oxidizing conditions between the HM and NNO buffers, i.e., a $\log_{10} f_{O_2}$ between -4 and -9 assuming magmatic temperatures near 1100 °C. The early and continuous crystallization of titanomagnetite and its abundance, the presence of silica- rather than Fe-enrichment trend (Springer, 1980b), and the limited Fe enrichment in olivine and pyroxene correlate with the results of experimental crystallization studies of basalts under similar oxidizing conditions (Roeder and Osborn, 1966; Presnall, 1966; Osborn, 1979). The limited Fe enrichment in olivine and pyroxene from pyroxenite to gabbro with plagioclase of $>An_{60}$ indicates a decrease in oxygen fugacity of one to two log fugacity units (Speidel and Os-

born, 1967) during crystallization of over 90% of the complex. The high values and range in Mg/(Mg + Fe) for calcic amphibole and biotite are also consistent with crystallization under similar oxidizing conditions (Wones and Eugster, 1965; Helz, 1973). Initially high water activity as well as high f_{O_2} characterize the magmatic crystallization of ultramafic-mafic rocks in the petrotectonic association of the Klamath Mountains and western Sierra Nevada (Snoke et al., 1982).

Compositional discontinuities in Mg/(Mg + Fe) for olivine and pyroxene as well as for calcic amphibole and biotite—all occurring at a plagioclase composition of near An_{60}—coincide with deformation of the complex. Lack of a similar discontinuity in plagioclase composition suggests that a significant temperature decrease did not accompany this deformation. It is proposed that the initial deformational event involved fracturing of the Pine Hill complex and adjacent country rock such that interaction of the fluid phase in the country rock and crystallizing magma occurred. This interaction involved a loss of fluid from the residual magma and resulted in a lower oxygen fugacity in the magma, reflected by an abrupt decrease in Mg/(Mg + Fe) of the mafic silicates. The fine-grained gabbro of the mixed zone possibly reflects rapid crystallization due to the loss of fluid phase from the magma.

The presence of calcic amphibole and biotite in the Pine Hill complex indicates that water was present in the parent magma. Melting relations of basalts indicate that at a total pressure of 3 kbar and under water-saturated (Yoder and Tilley, 1962) as well as water-undersaturated (P_{H_2O} and $0.6P_{total}$, Holloway and Burnham, 1972) conditions, calcic amphibole would be a liquidus phase; however, at a total pressure of <1.5 kbar, it would be a solidus phase. Regardless of the total pressure, if the crystallizing liquid does not at some time contain the minimum water content ($\geq 3.0\%$, Burnham, 1979) required for the coexistence of calcic amphibole and silicate melt, calcic amphibole would not crystallize from the magma. The absence of primary calcic amphibole as well as primary biotite in the Pine Hill complex is attributed to a low initial water content in the magma. As the water content of trapped intercumulus magma would increase with crystallization, the minimum water content required for the crystallization of calcic amphibole and biotite would be reached. Whether this intercumulus phase was largely a silicate melt or hydrous fluid phase during the crystallization of these hydrous minerals is not known. Prior to deformation of the complex, the Mg/(Mg + Fe) values of the mafic silicates exhibit the relationship bio > aug > opx > amph > ol; after deformation, aug > opx $\simeq$ bio $\simeq$ amph > ol. The relationship aug > amph > bio is common in plutonic igneous rocks in which calcic amphibole and biotite crystallized directly from the magma (Gilbert et al., 1982; Speer, 1984) even under oxidizing conditions between the NNO and HM buffer curves (Czamanske and Wones, 1973). A silicate melt— i.e., trapped intercumulus magma—may have been in equilibrium with crystallizing hydrous minerals after deformation but not before.

Magma composition

Most ultramafic to dioritic intrusive complexes in the Klamath Mountains and western Sierra Nevada, California, have been characterized by a multistage differentiation-emplacement model involving up to three parent magmas: (1) a primitive mafic basalt differentiating to dunite, wehrlite, gabbro, diorite, (2) a wet high-Al basalt differentiating to hornblende gabbro and diorite and then to tonalite, and (3) a tonalite (Snoke et al., 1981). In contrast to most complexes in this petrotectonic association, there are neither younger tonalitic rocks nor large amounts of hornblende gabbro and diorite associated with the Pine Hill intrusive complex. The rocks of Pine Hill complex correlate closely with the early ultramafic-gabbroic-dioritic rocks of these complexes. This feature suggests that the magmas from which the tonalitic rocks and hornblende gabbro and diorite were derived were commonly emplaced at the same locus along with the earlier primitive mafic basalt, but were generated separately from the primitive mafic basalt. The dunite-wehrlite-gabbro-diorite association of these complexes is similar to the dunite-wehrlite-gabbro association of the Alaskan-type complexes (James, 1971; Snoke et al., 1981, 1982). Characteristics of the Pine Hill complex similar to those of the Alaskan-type complexes are (1) olivine clinopyroxenite and clinopyroxenite that are gradational into gabbro with plagioclase of $>An_{90}$; (2) layering of titanomagnetite in clinopyroxenite and gabbro with plagioclase of $>An_{85}$, plus an overall abundance of titanomagnetite; (3) patches of pegmatitic clinopyroxenite and gabbro with plagioclase of $>An_{85}$; (4) igneous layering in gabbro with plagioclase of $>An_{85}$, produced by pseudosedimentary magmatic processes; (5) syncrystallization and subsolidus deformation involving flowage and brecciation of cumulates; (6) primary minerals that comprise olivine (Fo_{77} to Fo_{41}), Ca-rich pyroxene, Ca-poor pyroxene (absent in pyroxenite and gabbro with plagioclase of $>An_{85}$), titanomagnetite (subsolidus oxidation-exsolution to titaniferous magnetite, ilmenite, and pleonaste), calcic plagioclase, and late-crystallizing calcic amphibole with low SiO_2 and high Al_2O_3; (7) alkali feldspar–cordierite hornfels facies contact metamorphism in adjacent country rock (Taylor, 1967); and (8) emplacement into an orogenic tectonic environment. The major difference between the Pine Hill complex and the Alaskan-type complexes is the former's lack of dunite, which precludes the presence of chromian spinel and olivine $>Fo_{77}$.

Mineralogical similarities between the Pine Hill complex and plutonic rocks from island arcs (Aleutian, Lesser Antilles) and ophiolites (Troodos) probably indicate that conditions operating during crystallization of the parent basaltic magmas were similar. Compositional differences in parent basaltic magmas exist among these plutonic rocks, but are not reflected in their mineralogy adequately

to differentiate among them. For example, the mineralogy and major-element chemistry of ejected plutonic blocks in the Lesser Antilles island arc are similar to those of Pine Hill gabbro with plagioclase $>An_{85}$. The chemical composition of the parent basaltic magma for which these blocks, as well as associated basaltic andesitic volcanic rock, formed (Lewis, 1973a; Arculus and Wills, 1980) is markedly distinct from that calculated for the Pine Hill complex (Springer, 1980b). The absence of large amounts of silica-rich (i.e., $>50\%$ SiO_2) fractionation products and the relative amounts of fractionation products in the Pine Hill complex negate the hypothesis that this complex was a major source of andesitic magma.

A low-alkali, high-Ca olivine tholeiite similar in composition to the calculated chemical composition of the Pine Hill complex has been proposed as the parent magma for lavas and dikes on the Isle of Skye, Hebridean dikes and sills, and possibly the Cuillins and Rhum layered basic intrusions (Drever and Johnston, 1966; Donaldson, 1977). This olivine tholeiite, which is possibly related to the early stages in the development of a mid-oceanic ridge (Donaldson, 1977) is possibly correlative to the primitive mafic basalt of Snoke et al. (1981).

In the context of the western Sierra Nevada, the parent magma for the Pine Hill complex was probably generated within an island arc (Snoke et al., 1982). A similar origin is proposed for the gabbrodiorite plutons of the nearby Smartville complex (Beard and Day, 1987), whose age and mineralogy correlate closely with the Pine Hill complex.

SUMMARY

1. Crystallization in the Pine Hill intrusive complex can be divided into (1) crystallization directly from the magma, (2) crystallization of magma trapped within cumulates and closed to the main magma body, and (3) late crystallization involving a reaction of the primary minerals with a residual hydrous phase. Cumulus minerals exhibit the sequence ol + aug, ol + aug + mt, ol + aug + mt + pl, ol + aug + mt + pl + opx (inverted from pig), aug + mt + pl + opx (inverted from pig) $\pm$ qz. Intercumulus minerals include plagioclase in pyroxenite and partial rims of Ca-poor pyroxene on olivine. Late crystallization resulted in the formation of calcic amphibole and biotite.

2. Prior to complete solidification of the Pine Hill magma ($>90\%$ crystallized), mafic silicates exhibit limited Fe enrichment, whereas plagioclase shows a compositional variation of An_{95} to An_{60}. Near plagioclase of An_{60}, the mafic silicates show an abrupt decrease in Mg/(Mg + Fe), followed by limited Fe enrichment over the plagioclase composition range of An_{60} to An_{32}. Mg/(Mg + Fe) values for the mafic silicates prior to crystallization of plagioclase of An_{60} show bio > aug > opx > mph > ol, whereas at plagioclase of $<An_{60}$, the relationship is aug > opx $\simeq$ amph $\simeq$ bio > ol. This compositional discontinuity in the mafic silicates coincides with deformation of the com-

plex. Fracturing of the complex and adjacent country rock allowed the fluid phase in the country rock to gain access to the crystallizing magma, resulting in a decrease in the oxygen fugacity of the crystallizing magma.

3. Contact-metamorphic mineral assemblages and the crystallization sequence of primary minerals indicate a load pressure of <3 kbar during magmatic crystallization. Temperatures of magmatic crystallization were near 1100 °C, based on pyroxene geothermometry. High initial values of oxygen fugacity, i.e., between the HM and NNO buffer curves, in the Pine Hill magma allowed the early and abundant crystallization of titanomagnetite. A limited Fe-enrichment trend in the mafic silicates and a limited silica-enrichment trend in the magma indicate that oxygen fugacity probably decreased less than two log units during crystallization of over 90% of the complex.

4. Comparison of crystallization sequences and mineral variation in the Pine Hill complex to those in complexes of the Klamath Mountains and western Sierra Nevada, California, petrotectonic association, Alaskan-type complexes, ophiolites, and island-arc plutonism shows distinct similarities, largely indicative of similar conditions of crystallization. The Pine Hill magma, a low-alkali, high-Ca olivine tholeiite, was generated and emplaced in an island-arc environment.

REFERENCES CITED

Allen, C.R. (1975) The petrology of a portion of the Troodos plutonic complex, Cyprus. Ph.D. thesis, Cambridge University, Cambridge, England.

Anderson A.T. (1968) Oxidation of the LaBlache Lake titaniferous magnetite deposit, Quebec. Journal of Geology, 76, 528–547.

Arculus, R.J., and Wills, K.J.A. (1980) The petrology of plutonic blocks and inclusions from the Lesser Antilles island arc. Journal of Petrology, 21, 743–799.

Beard, J.S., and Day, H.W. (1987) The Smartville intrusive complex, Sierra Nevada, California: The core of a rifted volcanic arc. Geological Society of America Bulletin, 99, 779–791.

Bence, A.E., and Albee, A.L. (1968) Empirical correction factors for the electron microanalysis of silicates and oxides. Journal of Geology, 76, 382–403.

Best, M.G., and Mercy, E.L.P. (1967) Composition and crystallization of mafic minerals in the Guadalupe igneous complex, California. American Mineralogist, 52, 436–474.

Buddington, A.F., and Lindsley, D.H. (1964) Iron-titanium oxide minerals and synthetic equivalents. Journal of Petrology, 5, 310–357.

Burnham, C.W. (1979) The importance of volatile constituents. In H.S. Yoder, Jr., Ed., The evolution of the igneous rocks. Princeton University Press, Princeton, New Jersey.

Carmichael, I.S.E. (1967) the iron-titanium oxides of salic volcanic rocks and their associated ferromagnesian silicates. Contributions to Mineralogy and Petrology, 14, 36–64.

Czamanske, G.K., and Wones, D.R. (1973) Oxidation during magmatic crystallization, Finnmarka complex, Oslo area, Norway: Part 2, the mafic silicates. Journal of Petrology, 14, 349–380.

Donaldson, C.H. (1977) Petrology of anorthite-bearing gabbroic anorthosite dykes in northwest Skye. Journal of Petrology, 18, 595–620.

Drever, H.I., and Johnston, R. (1966) A natural high-lime silicate liquid more basic than basalt. Journal of Petrology, 7, 414–420.

Gilbert, M.C., Helz, R.T., Popp, R.K., and Speer, F.S. (1982) Experimental studies of amphibole stability. Mineralogical Society of America Reviews in Mineralogy, 9B, 229–278.

Hamilton, D.L., Burnham, C.W., and Osborn, E.F. (1964) The solubility of water and effects of oxygen fugacity and water content on crystallization in mafic magmas. Journal of Petrology, 5, 21–39.

Helz, R.T. (1973) Phase relations of basalts in their melting range of P_{H_2O} = 5 kb as a function of oxygen fugacity: Part I. Mafic phases. Journal of Petrology, 14, 249–302.

Holloway, J.R., and Burnham, C.W. (1972) Melting relations of basalt with equilibrium water pressure less than total pressure. Journal of Petrology, 13, 1–29.

Irvine, T.N. (1980) Magmatic density currents and cumulus processes. American Journal of Science, 280-A, 1–58.

James, O.B. (1971) Origin and emplacement of the ultramafic rocks of the Emigrant Gap area, California. Journal of Petrology, 12, 523–560.

Jorgenson, D.B. (1979) Textural banding in igneous rocks: An example from southwestern Oregon. American Mineralogist, 64, 527–530.

Kehlenbeck, M.M. (1972) Deformation textures in the Lac Rouvray anorthosite mass. Canadian Journal of Earth Sciences, 9, 1087–1098.

Kretz, Ralph. (1982) Transfer and exchange equilibria in a portion of the pyroxene quadrilateral as deduced from natural and experimental data. Geochimica et Cosmochimica Acta, 46, 411–421.

Leake, B.E. (1978) Nomenclature of amphiboles. American Mineralogist, 63, 1023–1052.

Lewis, J.F. (1973a) Petrology of the ejected plutonic blocks of the Soufriere volcano, St. Vincent, West Indies. Journal of Petrology, 14, 81–112.

——— (1973b) Mineralogy of the ejected plutonic blocks of the Soufriere volcano, St. Vincent: Olivine, pyroxene, amphibole and magnetite paragenesis. Contributions to Mineralogy and Petrology, 38, 197–220.

Lindsley, D.H. (1976) The crystal chemistry and structure of oxide minerals as exemplified by the Fe-Ti oxides. Mineralogical Society of America Reviews in Mineralogy, 3, L1–60.

——— (1983) Pyroxene thermometry. American Mineralogist, 68, 477–493.

Lindsley, D.H., and Andersen, D.J. (1983) A two-pyroxene thermometer. Proceedings of the Thirteenth Lunar and Planetary Science conference, Part 2. Journal of Geophysical Research, 88, Supplement, A887–A906.

Lindsley, D.H., and Spencer, K.J. (1982) Fe-Ti oxide geothermometry: Reducing analyses of coexisting Ti-magnetite (Mt) and ilmenite (Ilm). EOS, 63, 471.

McBirney, A.R., and Noyes, R.M. (1979) Crystallization and layering of the Skaergaard intrusion. Journal of Petrology, 20, 487–554.

Moore, A.C. (1973) Studies of igneous and tectonic textures and layering in rocks of the Goose Pike intrusion, central Australia. Journal of Petrology, 14, 49–79.

Morrison, D.A., Maczuga, D.E., Phinney, W.C., and Ashwal, L.D. (1986) Stratigraphy and petrology of the Mulcahy Lake layered gabbro: An Archean intrusion in the Wabigoon subprovince, Ontario. Journal of Petrology, 27, 303–341.

Morse, S.A. (1980) Basalts and phase diagrams: An introduction to the quantitative use of phase diagrams in igneous petrology. Springer-Verlag, New York.

Moseley, David. (1984) Symplectic exsolution in olivine. American Mineralogist, 69, 139–153.

Osborn, E.F. (1979) The reaction principle. In H.S. Yoder, Jr., Ed., The evolution of the igneous rocks, p. 133–169. Princeton University Press, Princeton, New Jersey.

Otten, M. T. (1984) The origin of brown hornblende in the Artfjallet gabbro and dolerites. Contributions to Mineralogy and Petrology, 86, 189–199.

Presnall, D.C. (1966) The join forsterite–diopside–iron oxide and its bearing on the crystallization of basaltic and ultramafic magmas. American Journal of Science, 264, 753–809.

Robinson, Peter, Ross, M., Nord, G.L., Jr., Smyth, J.R., and Jaffe, H.W. (1977) Exsolution lamellae in augite and pigeonite: Fossil indicators of lattice parameters at high temperature and pressure. American Mineralogist, 62, 857–873.

Roeder, P.L., and Osborn, E.F. (1966) Experimental data for the system $MgO-FeO-Fe_2O_3-CaAl_2Si_2O_8-SiO_2$ and their petrologic implications. American Journal of Science, 264, 428–480.

Rucklidge, John, and Gasparrini, E.L. (1969) Specifications of a computer program for processing electron micro-probe analytical data: EMPADR VII. Department of Geology, University of Toronto, Toronto, Ontario, Canada.

Saleeby, J.B. (1982) Polygenetic ophiolite belt of the California Sierra Nevada: Geochronological and tectonostratigraphic development. Journal of Geophsyical Research, 87, 1803–1824.

Smith, J.V. (1974) Feldspar minerals, vols. 1 and 2. Springer-Verlag, New York.

Snoke, A.W., Quick, J.E., and Bowman, H.R. (1981) Bear Mountain igneous complex, Klamath Mountains, California: An ultrabasic to silicic calc-alkaline suite. Journal of Petrology, 22, 501–552.

Snoke, A.W., Sharp, W.D., Wright, J.E., and Saleeby, J.B. (1982) Significance of mid-Mesozoic peridotitic to dioritic complexes, Klamath Mountains–western Sierra Nevada, California. Geology, 10, 160–166.

Speer, J.A. (1984) Micas in igneous rocks. Mineralogical Society of America Reviews in Mineralogy, 13, 299–356.

Speidel, D.H., and Osborn, E.F. (1967) Element distribution among coexisting phases in the system $MgO-FeO-Fe_2O_3-SiO_2$ as a function of temperature and oxygen fugacity. American Mineralogist, 52, 1139–1152.

Spencer, K.J., and Lindsley, D.H. (1981) A solution model for coexisting iron-titanium oxides. American Mineralogist, 66, 1189–1201.

Springer, R.K. (1974) Contact metamorphosed ultramafic rocks in the western Sierra Nevada foothills, California. Journal of Petrology, 15, 160–195.

——— (1980a) Geology of the Pine Hill intrusive complex, a layered gabbroic body in the western Sierra Nevada foothills, California: Summary. Geological Society of America Bulletin, pt. I, 91, 381–385.

——— (1980b) Geology of the Pine Hill intrusive complex, a layered gabbroic body in the western Sierra Nevada foothills, California. Geological Society of America Bulletin, pt. II, 91, 1536–1626.

Springer, R.K., and Craig, J.R. (1975) Sulfide mineralogy of metamorphosed ultramafic rocks, western Sierra Nevada foothills, California. Economic Geology, 70, 1478–1483.

Stormer, J.C., Jr. (1983) The effects of recalculation on estimates of temperature and oxygen fugacity from analyses of multicomponent iron-titanium oxides. American Mineralogist, 68, 586–594.

Tarney, J. (1969) Epitaxic relations between coexisting pyroxenes. Mineralogical Magazine, 37, 115–122.

Taylor, H.P., Jr. (1967) The zoned ultramafic complexes of southeastern Alaska. In P.J. Wyllie, Ed., Ultramafic and related rocks, p. 97–121. Wiley, New York.

Wager, L.R., and Brown, G.M. (1967) Layered igneous rocks. W. H. Freeman, San Francisco.

Wager, L.R., Brown, G.M., and Wadsworth, W.J. (1960) Types of igneous cumulates. Journal of Petrology, 1, 73–85.

Wells, P.R.A. (1977) Pyroxene thermometry in simple and complex systems. Contributions to Mineralogy and Petrology, 62, 129–139.

Wones, D.R., and Eugster, H.P. (1965) Stability of biotite: Experiment, theory, and application. American Mineralogist, 50, 1228–1272.

Wood, B.J., and Banno. S. (1973) Garnet-orthopyroxene and orthopyroxene-clinopyroxene relationships in simple and complex systems. Contributions to Mineralogy and Petrology, 42, 109–124.

Yoder, H.S., Jr., and Tilley, C.E. (1962) Origin of basaltic magma: An experimental study of natural and synthetic rock systems. Journal of Petrology, 3, 342–532.